CHASE-ESCAPE WITH CONVERSION AS A MULTIPLE SCLEROSIS LESION MODEL

EMMA BAILEY, ERIN BECKMAN, SARAÍ HERNÁNDEZ-TORRES, MATTHEW JUNGE, AANJANEYA KUMAR, ANN LEE, DANNY LI, TAHDA QUEER, ALISHER RAUFOV, LILY REEVES, AND OMER RONDEL

Abstract. We introduce conversion to the stochastic process known as chase-escape in an effort to model aspects of inflammatory damage from multiple sclerosis. We prove monotonicity results for aggregate damage for the model on the positive integers, trees, stars, and the complete graph. Additionally, we establish the existence and asymptotic order of a phase transition on bounded degree graphs with a non-trivial site percolation threshold.

1. Introduction

Multiple sclerosis (MS) is a chronic disease characterized by lesions of damaged white matter in the central nervous system (CNS). Roughly speaking, MS lesions are formed when inflammatory T-cells recruit macrophages and B-cells to attack myelin in the CNS. The process is eventually suppressed and halted by regulatory T-cells, often leaving behind a lesion of permanently damaged CNS tissue [7, 18]. A prominent issue with studying MS is that it is extremely difficult to obtain dynamical information from patients or even animal models [16].

Mathematical models have the potential to provide unique insights [29]. In their survey article, Weatherly et al. describe various MS modeling attempts [29]. Lombardo et al. introduced an ordinary differential equations (ODE) model for the interactions among macrophages, chemoattractants and destroyed oligodendrocytes [19]. Kotelnikova et al. introduced a different ODE model describing interactions among axons and macrophages [16]. They showed that their model can be adjusted to match different disease courses in MS patients. In [23], Moise and Avner developed a more comprehensive model of lesion formation. It involved a complex system of differential equations involving dozens of agents and a three-dimensional space variable. Their model exhibited quantitative agreement with clinical data that measured total lesion volume in MS patients [5, 20]. Travaglini recently developed a similar reaction-diffusion equation based approach [22]. Schoonheim et al. proposed a network-based approach to describe MS dynamics and postulated that disease impairment heightens with "network collapse" i.e., when important connective regions accrue too much damage [25].

The aforementioned models are deterministic. However, lesion formation appears to be partly driven by local random interactions [19]. Stochastic spatial models for remyelination in the CNS were proposed in [11, 28]. Kim et al. introduced a

Part of this research was conducted during a Mathematical Research Intensive supported by NSF DMS Grant 2238272 that also partially supports MJ, AL, DL, tq, AR, and OR. SHT acknowledges support from UNAM-PAPIIT grant IA103724. LR is partially supported by the NSF MSPRF Award DMS-2303316. Thanks to Josh Cruz for assistance with Figure 2.

programmed cell death model on random networks [14] that was later applied to MS lesion formation [27, 21]. Their simulation results suggested that preemptively killing cells through a process called apoptosis can limit total damage.

We model the interplay between inflammatory T-cells and regulatory T-cells by generalizing a stochastic growth model known as chase-escape to include spontaneous conversion to account for the arrival of regulatory cells. This line of inquiry aligns with recent experimental gene therapies to treat MS by boosting the production of regulatory T-cells [12]. The two questions we seek to address are:

(1) Is CNS tissue damage monotone in the inflammatory and suppression rates?
(2) Does tissue damage exhibit a phase transition?

Question (1) is not apriori obvious, since rapid inflammation might trigger more vigorous suppression, resulting in less damage as seen in the model from [27]. The basic idea of Question (2) is characterizing conditions that allow lesions to reach macroscopic size.

Since we approach these questions with full rigor, our model is a dramatic oversimplification. Nonetheless, our inquiry lies at the theoretical forefront of stochastic growth models. Our primary aim is to advance theoretical tools that may one day be sophisticated enough to capture more salient features of MS.

1.1. **Model definition.** In our model, inflammatory r-particles "escape" to and damage healthy w-sites while being "chased" and suppressed by regulatory b-particles. We will refer to sites with r- or b-particles as red or blue, respectively and healthy w-sites as white. Spontaneous "conversion" of red to blue sites represents the arrival of regulatory cells that halt inflammation. Thus, red sites represent cells with active inflammation, and blue sites represent damaged cells at which there is no longer inflammation. To distinguish between the two mechanisms by which a blue particle can occupy a site, either by blue spreading to a site through chasing a red particle or by a red particle converting to blue, we will sometimes call the former *chase* or *predation* and the latter we will refer to as *conversion*.

Formally, *chase-escape with conversion* takes place on a locally finite graph G in which vertices are in one of the three states $\{w, r, b\}$. Adjacent vertices in states (r, w) transition to (r, r) according to independent Poisson processes with rate λ. Each vertex in state r transitions to state b according to an independent Poisson process with rate α. Adjacent (b, r) vertices transition to (b, b) according to independent rate 1 Poisson processes. The standard initial configuration has the root vertex x_0 in state r and all other vertices in state w. See Figure 1 for a visual summary of the dynamics and Figure 2 for some examples of the initial configuration on various graphs. Note that the process is well-defined on any locally finite graph since the memoryless property of Poisson processes allows us to update the always finite configuration of red and blue sites in a Markovian manner.

The special case $\alpha = 0$ corresponds to the well-studied *chase-escape* model introduced by ecologists Keeling, Rand, and Wilson [13, 24] to study parasite-host relations. Further work has reinterpreted the dynamics as models for: predator-prey systems, rumor scotching, infection spread, and malware repair in a device network [4, 3, 6, 10, 9]. Note that for chase-escape, both red and blue sites must be present in the initial configuration, and this is usually implemented by adding an additional vertex in state b attached to x_0. Also note that we could add a third parameter β to modify the spreading rate of blue to obtain a larger class of models.

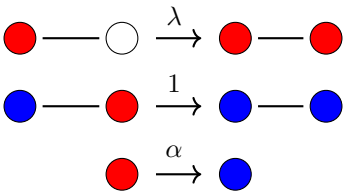

FIGURE 1. Chase-escape with conversion dynamics.

For example, setting $\beta = 0$ would yield the classical SIR model of infection spread [8]. We believe our results still hold for general $\beta > 0$. However, since conversion is the main novelty, we opt for a simpler presentation with β fixed at 1.

For chase-escape with conversion on G with site x_0 initially in state r, let $X = X(G, x_0, \lambda, \alpha)$ be the number of sites in state b when the process eventually fixates. We adopt the convention that $X = \infty$ if the process never fixates. Much of the chase-escape literature has focused on the critical red spreading rate when G is an infinite graph. The analogue for chase-escape with conversion is

$$\lambda_c(\alpha) = \lambda_c(\alpha, G, x_0) \coloneqq \sup\{\lambda \colon \mathbf{P}_{\lambda,\alpha}(X < \infty) = 1\}, \tag{1}$$

above which X is infinite with positive probability [9]. This definition could be adapted to growing sequences of finite graphs as was done for chase-escape in [2].

Another intriguing feature of chase-escape is the apparent difficulty to prove monotonicity in λ. Recall that a nonnegative random variable X' is stochastically smaller than another nonnegative random variable X (denoted $X' \preceq X$) if and only if there is a coupling such that $X' \leq X$ almost surely, or equivalently $\mathbf{P}(X' \geq a) \leq \mathbf{P}(X \geq a)$ for all $a \geq 0$. When G contains cycles, it remains an open problem in most natural settings (for example $\mathbb{Z}^2$ [17]) to prove stochastic monotonicity of X in λ. Although faster spread of red particles is believed to cause red to reach more sites, there is the offsetting effect that more red sites means more opportunities for blue to spread. A similar effect happens with conversion. Faster conversion should reduce X, but more red conversion means fewer red sites for blue to chase.

1.2. **Results.** We are interested in whether or not X is monotone in λ and α. When $\alpha = 0$, it is straightforward to see that X is monotone in λ on trees. However, when $\alpha > 0$, the question of monotonicity in λ is less clear, even on trees, because speeding up red introduces more conversion opportunities.

Let $\mathbb{N}$ denote the positive integers $1, 2, \ldots$ with root $x_0 = 1$, S_n denote the star graph with root vertex x_0 attached to n leaf vertices, $\mathcal{T}$ denote a locally finite tree rooted at x_0, and K_n denote the complete graph on n vertices, labeled $1, 2, \ldots, n$ with root $x_0 = 1$. See Figure 2. Note that $\mathbb{N}$ and S_n are special cases of tree graphs.

We say that the number of damaged sites in chase-escape with conversion, X, is monotone in λ if $X(G, x_0, \lambda', \alpha) \preceq X(G, x_0, \lambda, \alpha)$ for $\lambda' \leq \lambda$, and X is monotone in α if $X(G, x_0, \lambda, \alpha') \preceq X(G, x_0, \lambda, \alpha)$ for $\alpha' \geq \alpha$. We say that X is monotone in n for the process on S_n if $X(S_{n'}, \lambda, \alpha, x_0) \preceq X(S_n, \lambda, \alpha, x_0)$ for all $n' \leq n$, and similarly for monotonicity in n for the process on K_n.

Theorem 1. *The number of damaged sites X in chase-escape with conversion:*

(i) Is monotone in α for $\mathcal{T}, \mathbb{N}$, S_n, and K_n.
(ii) Is monotone in λ for $\mathbb{N}$, S_n, and K_n.

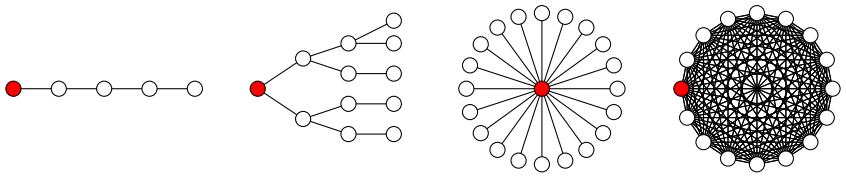

FIGURE 2. From left to right: The positive integers $1, \dots, 5$, a tree with 12 vertices, the star graph S_{20}, and the complete graph K_{16}. The root x_0 is shaded red in each example.

(iii) Is monotone in n for S_n and K_n.

We also prove that $\lambda_c(\alpha)$, defined at (1), is non-trivial and pin down its leading order on infinite graphs with bounded degree and non-trivial site percolation threshold. Let G be an infinite graph with root x_0. Recall that in Bernoulli site percolation, each vertex is open independently with probability p and otherwise closed. The percolation critical value is

$$p_c = p_c(G, x_0) := \inf\{p \colon \mathbf{P}_p(x_0 \in \text{an infinite open cluster}) > 0\}.$$

Here a cluster is a maximal component of open vertices connected to one another by at least one edge. We prove that there is a non-trivial phase transition whenever p_c is non-trivial and, in doing so, obtain the first-order growth of $\lambda_c(\alpha)$. Note that for a non-negative function f we write $f(x) = \Theta(x)$ if there exist constants $c, C > 0$ such that $c < f(x)/x < C$ for all large x.

Theorem 2. *Fix $\alpha > 0$. Suppose that G is an infinite graph with maximum degree $3 \le d < \infty$ and $p_c(G, x_0) < 1$. It holds that*

$$\frac{\alpha}{d-2} \le \lambda_c(\alpha) \le \frac{d+\alpha}{1 - p_c(G, x_0)^{1/d}}.$$

Thus, $\lambda_c(\alpha) = \Theta(\alpha)$.

Examples of graphs for which Theorem 2 applies are infinite lattices and regular trees.

1.3. **Further questions.** We conjecture that X is monotone in λ on trees and $\mathbb{Z}^d$. It would be worthwhile to study chase-escape with conversion on finite random networks whose topologies more closely resemble neuron structures, such as Erdős-Rényi and random spatial graphs [2, 27]. A central question in chase-escape on $\mathbb{Z}^2$ is proving that $\lambda_c(0) < 1$ [26, 9], or, even better, that $\lambda_c(0) < 1/2$ as conjectured in [17]. With the introduction of conversion, one could seek estimates on $\lambda_c(\alpha)$. For example, does $\lambda_c(\alpha)/\alpha \to C$ for some $C > 0$ as $\alpha \to \infty$? Alternatively, it would be interesting to investigate the dual critical value $\alpha_c(\lambda) := \inf\{\alpha \colon \mathbf{P}_{\lambda,\alpha}(X < \infty) = 1\}$.

In Figure 3, we provide simulation estimates of $\lambda_c(1) \approx 1.975$ and $\alpha_c(1) \approx 0.275$ for the process on $\mathbb{Z}^2$. The curves in the figure also support our monotonicity on $\mathbb{Z}^d$ conjecture. See Figure 4 for snapshots of the process on $\mathbb{Z}^2$. Another interesting variation would allow for an increasing conversion rate $\alpha(t)$ that models increased immune response over time.

A future project is to develop a data set using MRI data consisting of the spatial structure of individual MS lesions. Since MRI data is broken down into cubic

millimeter boxes (known as voxels), storing a lesion's structure in $\mathbb{Z}^3$ would be natural. Such data could be used as benchmarks to compare models against. To our knowledge, none of the previously mentioned MS models have performed such benchmarking. The closest analogue is [23], which compared their models to studies that measured the total volume of lesions in participants [20], but this was non-spatial data.

1.4. **Proof Overview.** Theorem 1 is proven via explicit couplings that allow us to compare how X is sampled for different parameter choices. Seemingly obvious monotonicity can be difficult to prove. The proper framing is needed to obtain Theorem 1 and varies from graph to graph. For example, we find occasion to sample X in a non-Markovian manner using edge passage times (for $\mathcal{T}$ and part of the proof for $\mathbb{N}$), in a continuous time Markovian manner (for K_n), in a mixture of these two viewpoints for S_n, and as a discrete time Markov process (for part of the proof for $\mathbb{N}$).

For $\mathbb{N}$, we discretize the process by generalizing a jump chain construction from [1]. Conversion introduces new challenges. For example, the initial height of the jump chain is now random. To couple the starting locations of different jump chains, we use the passage time construction for trees. In the coupling, we must run the monotonically smaller process longer than its counterpart. Once the starting heights are coupled, comparing the evolution for different parameters is also more subtle due to conversion. Maintaining a working coupling requires the introduction of neutral flat steps to the jump chains.

Monotonicity for the star graph uses a pure death process along with a queue to assign the times for blue to reach the root from a given leaf. For K_n we use the framework introduced in [15] that reduces the dynamics to studying birth and death processes. Conversion introduces constant immigration to the previously pure birth process. The lower bound on $\lambda_c(\alpha)$ in Theorem 2 is proven using a first-moment bound that relies on red being unlikely to survive along a given path [2]. The upper bound uses a coupling with site-percolation that was introduced in [10].

1.5. **Organization.** We prove Theorem 1 by graph: Section 2 handles trees, Section 3 the positive integers, Section 4 stars, and Section 5 the complete graph. Section 6 proves Theorem 2.

2. Proof of Theorem 1: Trees

Fix a tree $\mathcal{T}$ with root x_0 as well as a value of λ. Let $\alpha' \geq \alpha$. We must prove that $X' \coloneqq X(\mathcal{T}, x_0, \alpha', \lambda) \preceq X(\mathcal{T}, x_0, \alpha, \lambda) =: X$. We will proceed by constructing the chase-escape with conversion process by assigning passage times to directed edges and vertices, then explaining how these times can be used to deduce the value of X i.e., that X is measurable with respect to these passage times. Specifically, we may partition X by

$$X = \sum_{n=0}^{\infty} |\mathcal{L}(n)| = 1 + \sum_{n=0}^{\infty} \sum_{x \in \mathcal{L}(n)} |\mathcal{I}(x)|$$

where $\mathcal{L}(n)$ denotes the set of vertices ever colored red at level n and $\mathcal{I}(x)$ denotes the set of children of x ever colored red. Note that given the tree structure, $\mathcal{L}(n+1) = \bigcup_{x \in \mathcal{L}(n)} \mathcal{I}(x)$. We will inductively define $\mathcal{L}(n)$ and $\mathcal{I}(x)$ using passage times.

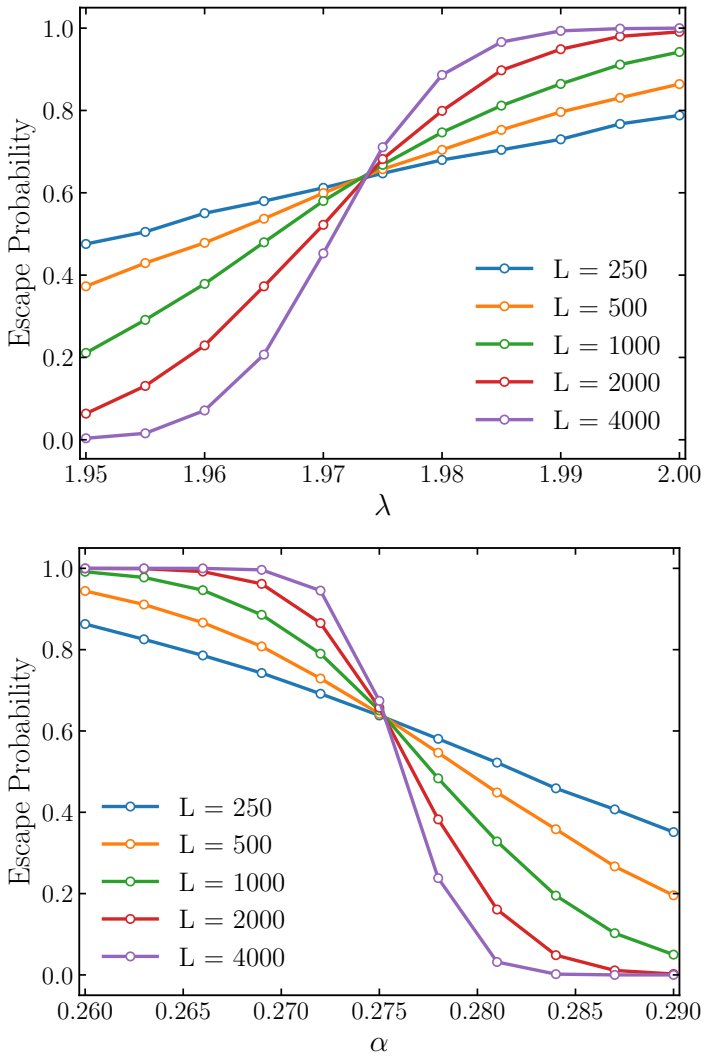

FIGURE 3. Simulations suggesting $\lambda_c(1) \approx 1.975$ (top) and $\alpha_c(1) \approx 0.275$ (bottom) for chase-escape with conversion on $\mathbb{Z}^2$. The process was run on two-dimensional tori with side lengths $L = 250, 500, 1000, 2000, 4000$, initializing all vertices on the bottom edge as blue and those vertices one level above as red. The curves interpolate between empirical estimates of the "Escape Probability", the probability that red reaches the top edge of the torus, averaged over 50,000 samples for each value of λ and α indicated by open circles on the curves. The intersection of the curves for the different values of L should be close to the true critical value, as in [17]. Note that we also see what looks like monotonicity of the escape probability in λ and α.

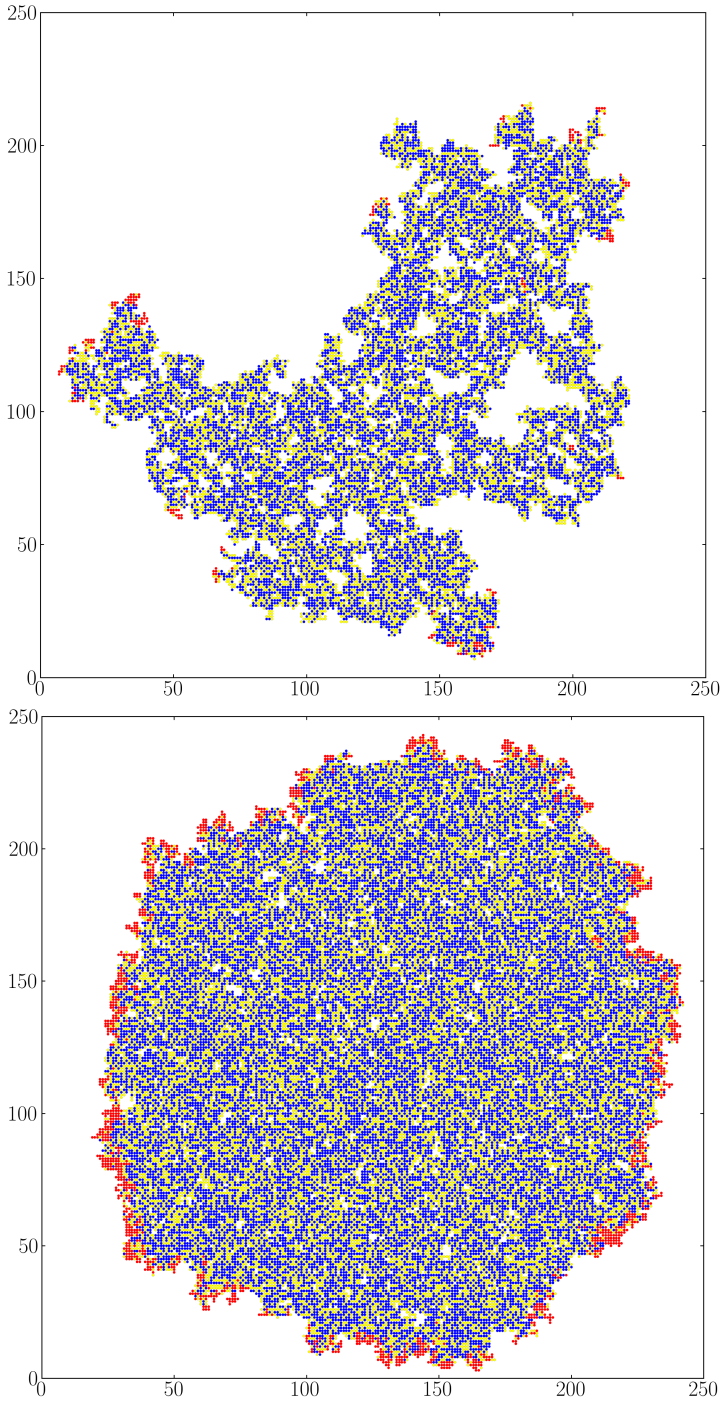

FIGURE 4. Sample realizations of the (still evolving) damaged region on a 250×250 box started with the central vertex in red and all other vertices in white. Sites that turned blue from conversion are colored yellow and those that turned blue from predation are colored blue. We set $\alpha = 1$ in both with $\lambda = 1.976$ (top) and $\lambda = 3$ (bottom).

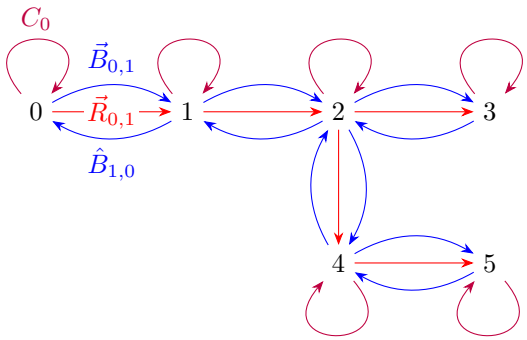

FIGURE 5. Directed edges representing the passage times $\vec{R}_{\hat{y},y}, \vec{B}_{\hat{y},y}, \hat{B}_{y,\hat{y}}$, and C_y. These are labeled for $\hat{y} = 0$ and are assigned similarly at the other vertices. On a tree, X is measurable with respect to these passage times.

It then suffices to show that $\mathcal{I}'(x) \subset \mathcal{I}(x)$ for all $x \in \mathcal{T}$ where $\mathcal{I}'(x)$ is defined analogously to $\mathcal{I}(x)$ for the coupled process with parameter $\alpha' \geq \alpha$.

Throughout the paper, we let $\text{Exp}(\mu)$ denote the exponential distribution with density function $\mu x^{-\mu x}$ for $x \geq 0$. We will use the notation $Y \sim \text{Exp}(\mu)$ to denote that Y is a random variable with this distribution. We proceed in two steps: first, describing the setup and then proving monotonicity.

2.1. **Setup.** Call $\hat{y} \in \mathcal{T}$ the *parent* of y if $\hat{y}$ shares an edge with y and lies on the geodesic path of edges connecting y to the root x_0. In this case, call y a *child* of $\hat{y}$. The *progeny* of y consists of all children of y, their children's children, and so on. Given $x \in \mathcal{T}$, define the subtree $\mathcal{T}(x)$ that includes vertices whose geodesic path to x excludes $\hat{x}$, i.e., $\mathcal{T}(x)$ includes x and all generations of its descendants. For each vertex $y \in \mathcal{T}(x)$, let $(x = x_1, x_2, \ldots, x_n = y)$ be the geodesic path of vertices between x and y. This path is simply (x) when $x = y$ and (x, y) when x and y are adjacent.

To each edge $\mathcal{E}_{\hat{y},y}$ we assign $(\vec{R}_{\hat{y},y}, \vec{B}_{\hat{y},y}, \hat{B}_{\hat{y},y}, C_y)$ consisting of four independent exponentially distributed random variables, which are also independent from those assigned to other edges. The values $\vec{R}_{\hat{y},y} \sim \text{Exp}(\lambda)$ and $\vec{B}_{\hat{y},y} \sim \text{Exp}(1)$ give the time it takes for red and blue, respectively, to spread from $\hat{y}$ to y. The value $\hat{B}_{\hat{y},y} \sim \text{Exp}(1)$ represents the time it takes for blue to spread from y to $\hat{y}$. Note that the tree structure ensures that red cannot spread from y to $\hat{y}$. Lastly, $C_y \sim \text{Exp}(\alpha)$ represents the conversion time at y. See Figure 5 for visual representation of these passage times as directed edges.

Given a vertex x and $y \in \mathcal{T}(x)$, define the infection times

$$T_{x,y} := \left(\sum_{i=1}^{n-1} \vec{R}_{x_i,x_{i+1}}\right) + C_y + \left(\sum_{i=1}^{n-1} \hat{B}_{x_{n-i+1},x_{n-i}}\right). \tag{2}$$

The times $T_{x,y}$ give how long it takes for x *to be infected from the conversion of* y: red spreads from x to y, the vertex y converts to blue, and then the sites along the geodesic from y to x turn blue by predation until ultimately predating x so it becomes blue. For each vertex x, this sequence of events can occur at most once,

for some y in the progeny $\mathcal{T}(x)$ (note that $T_{x,y}$ considers only the conversion of vertex y). Accordingly, we define:

$$T_x = \min\{T_{x,y} \colon y \in \mathcal{T}(x)\}.$$

Let $\mathbf{S}_x$ denote the *survival time of* x, that is, the time at which x first turns blue. We use the conventions that bold letters are in the units of global time as the process runs and that $\mathbf{S}_x$ is infinite if x never turns blue. Letting $(x_0, x_1, x_2, \dots, x_n = x)$ be the geodesic path of vertices from x_0 to x, define

$$\mathbf{R}_x := \vec{R}_{x_0,x_1} + \cdots + \vec{R}_{x_{n-1},x_n}$$

to be the time for red to reach x from x_0. We say that a vertex $x \in \mathcal{T}$ is of *generation* n if the geodesic path from x_0 to x contains $n+1$ vertices.

For generation 0, we have $\mathcal{L}(0) = \{x_0\}$. The root x_0 can only turn blue because one of its descendants (including itself) converted to blue and spread to x_0. Thus, we have

$$\mathbf{S}_{x_0} := T_{x_0}.$$

Letting $\mathcal{C}(x)$ denote the child vertices connected to the vertex x, the children of the root x_0 that are ever in state red are exactly those who turned red before x_0 turns blue, i.e.,

$$\mathcal{I}(x_0) \coloneqq \{x \in \mathcal{C}(x_0) \colon \vec{R}_{x_0,x} \le \mathbf{S}_{x_0}\}. \tag{3}$$

Given $\mathcal{L}(0), \dots, \mathcal{L}(n)$, $\mathbf{S}_x$ and $\mathcal{I}(x)$ for each $x \in \bigcup_{k \le n-1} \mathcal{L}(k)$, let us describe how to determine $\mathbf{S}_x$ and $\mathcal{I}(x)$ for each $x \in \mathcal{L}(n)$ and thus $\mathcal{L}(n+1)$.

Fix $x \in \mathcal{L}(n)$ and consider its parent $\hat{x} \in \mathcal{L}(n-1)$. Note that x turns blue either by predation from $\hat{x}$ or by infection from the conversion of one of its descendants (including itself). Thus, the survival time of x is given by

$$\mathbf{S}_x = (\mathbf{R}_x + T_x) \wedge (\mathbf{S}_{\hat{x}} + \vec{B}_{\hat{x},x}).$$

Thus, the set of children that x converts to red is given by

$$\mathcal{I}(x) := \{y \in \mathcal{C}(x) \colon \mathbf{R}_y \le \mathbf{S}_x\} \tag{4}$$

and

$$\mathcal{L}(n+1) = \bigcup_{x \in \mathcal{L}(n)} \mathcal{I}(x).$$

We obtain a partition $\{x_0\} \cup \bigcup_{n=0}^{\infty} \bigcup_{x \in \mathcal{L}(n)} \mathcal{I}(x)$ of vertices that are ever colored red. Using the memoryless property of the exponential distribution, this yields the following characterization of X

$$X = 1 + \sum_{n=0}^{\infty} \sum_{x \in \mathcal{L}(n)} |\mathcal{I}(x)|.$$

2.2. **Proof of monotonicity.** Fix $\alpha' \ge \alpha$, and define the analogous spreading times with the following couplings: $\vec{R}'_{\hat{y},y} = \vec{R}_{\hat{y},y}, \vec{B}'_{\hat{y},y} = \vec{B}_{\hat{y},y}, \hat{B}'_{y,\hat{y}} = \hat{B}_{y,\hat{y}}$, and $C'_y \le C_y$ with $C'_y \sim \mathrm{Exp}(\alpha')$. Using these coupled passage times and defining $\mathcal{I}'(x)$ and $\mathcal{L}'(n)$ analogously, we may sample X' by taking

$$X' = 1 + \sum_{n=0}^{\infty} \sum_{x \in \mathcal{L}'(n)} |\mathcal{I}'(x)|.$$

Using the convention that $\mathcal{I}(x) = \emptyset$ if $x \notin \bigcup_n \mathcal{L}(n)$, it suffices to show that $\mathcal{I}'(x) \subseteq \mathcal{I}(x)$ for all $x \in \mathcal{T}$. We will do this by induction. For the base case, we show that $\mathcal{I}'(x_0) \subseteq \mathcal{I}(x_0)$. Recall that the red and blue passage times are coupled to be equal. Hence, the first and third terms in (2) are the same in both systems:

$$\sum_{i=1}^{n-1} \vec{R}_{x_i,x_{i+1}} = \sum_{i=1}^{n-1} \vec{R}'_{x_i,x_{i+1}},$$
$$\sum_{i=1}^{n-1} \hat{B}_{x_{n-i+1},x_{n-i}} = \sum_{i=1}^{n-1} \hat{B}'_{x_{n-i+1},x_{n-i}}.$$

$C'_y \leq C_y$ implies $T'_{x,y} \leq T_{x,y}$ for all $y \in \mathcal{T}(x)$ and therefore $T'_x \leq T_x$ for all $x \in \mathcal{T}$. Thus, $\boldsymbol{S}'_{x_0} \leq \boldsymbol{S}_{x_0}$. Note that $\boldsymbol{R}_x = \boldsymbol{R}'_x$ for all $x \in \mathcal{T}$, so this ordering of the survival times imposes a more stringent condition at (3) for inclusion in $\mathcal{I}'(x_0)$ than in $\mathcal{I}(x_0)$. Thus, $\mathcal{I}'(x_0) \subseteq \mathcal{I}(x_0)$.

Suppose we have $\mathcal{I}'(v) \subset \mathcal{I}(v)$ for every $v \in \mathcal{T}$ of generation 0 to n. For any $x \in \mathcal{T}$ of generation $n+1$, its parent $\hat{x}$ is of generation n. The inclusion $\mathcal{I}'(x) \subset \mathcal{I}(x)$ trivially holds in the following scenarios:

- $x \notin \mathcal{I}(\hat{x})$: The induction hypothesis implies $x \notin \mathcal{I}'(\hat{x})$ so that $\mathcal{I}(x) = \mathcal{I}'(x) = \emptyset$.
- $x \notin \mathcal{I}'(\hat{x})$: Then $\mathcal{I}'(x) = \emptyset \subset \mathcal{I}(x)$.

Thus it remains to consider when $x \in \mathcal{I}(\hat{x}) \cap \mathcal{I}'(\hat{x})$. In this case, both $\mathcal{I}(\hat{x})$ and $\mathcal{I}'(\hat{x})$ are nonempty and so $\boldsymbol{S}_{\hat{x}}, \boldsymbol{S}'_{\hat{x}} < \infty$ almost surely. Recall that

$$\boldsymbol{S}_x = (\boldsymbol{R}_x + T_x) \wedge (\boldsymbol{S}_{\hat{x}} + \vec{B}_{\hat{x},x}),$$
$$\boldsymbol{S}'_x = (\boldsymbol{R}'_x + T'_x) \wedge (\boldsymbol{S}'_{\hat{x}} + \vec{B}'_{\hat{x},x}).$$

Since we have the equalities $\boldsymbol{R}_x = \boldsymbol{R}'_x$, $\vec{B}_{\hat{x},x} = \vec{B}'_{\hat{x},x}$, and the inequalities $T'_x \leq T_x$, $\boldsymbol{S}'_{\hat{x}} \leq \boldsymbol{S}_{\hat{x}}$, we can see that $\boldsymbol{S}'_x \leq \boldsymbol{S}_x$. Therefore, the condition in (4) is more stringent with $\boldsymbol{S}'_x$ than with $\boldsymbol{S}_x$ and so $\mathcal{I}'(x) \subseteq \mathcal{I}(x)$ as desired.

This proves that $\mathcal{I}'(x) \subseteq \mathcal{I}(x)$ for all $x \in \mathcal{T}$ and therefore that $X' \preceq X$ as desired.

Remark 3. *We have proven the stronger statement that the set of vertices* $\{x_0\} \cup \bigcup_{x \in \mathcal{T}} \mathcal{I}(x)$ *ever colored red is stochastically decreasing in* α.

Remark 4. *This construction of* X *highlights the difficulty in proving monotonicity in* λ. *Increasing* λ, *reduces the* $\vec{R}_{x,y}$ *passage times, and as a result, reduces both* $\mathbf{R}_x$ *and* $\boldsymbol{S}_x$. *Thus, both sides are reduced in the comparison in* (4).

Remark 5. *This argument does not generalize to graphs with cycles because the comparisons needed to determine which vertices are ever colored red are more complicated.*

3. Proof of Theorem 1: The positive integers

As observed in [1], a useful quantity for analyzing variants of the chase-escape process on the positive integers $\mathbb{N}$ is the *jump chain* $(Y_t)_{t \in \mathbb{N}}$. This discrete-time process tracks the number of (necessarily contiguous) red sites in front of the rightmost blue. For example, the jump chain corresponding to this configuration of red and blue on $\mathbb{N}$

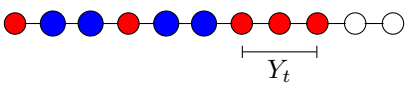

would have height 3. If, at the next transition, the configuration changed to

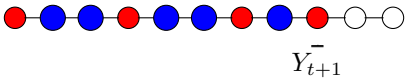

the jump chain would then have height 1. We emphasize that the values $t = 0, 1, \ldots$ are discrete and correspond to the (random) times at which the configuration changes. See [1] for a more formal description in the case of chase-escape.

For our purposes, an *active jump chain* is then described by a lattice path that:

- Starts at $(0, Y_0)$ for some $Y_0 \geq 0$.
- Consists of $+(1, 1)$ up-steps and $+(1, -j)$ down-steps for any $j \geq 1$.
- Is never negative and stops upon reaching 0.

If the jump chain is at (t, k), then the next step is to $(t+1, j)$, for $j \in \{0, 1, \ldots, k-1, k+1\}$, with probabilities $p_{k,j}$ where

$$p_{k,k+1} = \frac{\lambda}{1+\lambda+\alpha k}, \qquad p_{k,k-1} = \frac{1+\alpha}{1+\lambda+\alpha k},$$

and

$$p_{k,j} = \frac{\alpha}{1+\lambda+\alpha k} \qquad 0 \leq j \leq k-2.$$

The first term, $p_{k,k+1}$, is the probability that the rightmost red advances. The second term, $p_{k,k-1}$, is the probability that either the rightmost blue advances or the leftmost red (in the relevant connected component) converts to blue. The third term, $p_{k,j}$, is the probability that the red at distance $k - j$ from the rightmost red converts to blue. Reaching 0 corresponds to the rightmost red becoming blue, thus ending the possibility of red advancement.

The jump chain evolves until the stopping time $\kappa = \inf\{t \colon Y_t = 0\}$ with the convention that $\kappa = 0$ whenever $Y_0 = 0$. Let

$$U(n) = \#\{0 < t \leq \kappa \colon Y_t = Y_{t-1} + 1 \mid Y_0 = n\}$$

be the number of up-steps by the jump chain $(Y_t)_{t\in\mathbb{N}}$ starting with $Y_0 = n$.

One can start tracking the jump chain at any point from the appearance of the first blue on. Let N_t be the site of the rightmost red at time t and M_t be the site of the rightmost blue at time t with the convention that $N_t = M_t$ if the rightmost non-white site is blue, the jump chain construction yields the following characterization of X on the positive integers $\mathbb{N}$, rooted at $x_0 = 1$.

Lemma 6. *For any time t when blue is present in the system, $X(\mathbb{N}, x_0, \alpha, \lambda) \stackrel{d}{=} N_t + U(N_t - M_t)$.*

In particular, let γ be the time of the first conversion from red to blue and denote $N := N_\gamma$ and $M := M_\gamma$, that is, M is the first site to convert to blue. Lemma 6 implies that $X(\mathbb{N}, x_0, \alpha, \lambda) \stackrel{d}{=} N + U(N - M)$.

We will prove that X is monotone in α and λ simultaneously by coupling the jump chains corresponding to parameter choices $\alpha \leq \alpha'$ and $\lambda \geq \lambda'$. Let $X' = X'(\mathbb{N}, x_0, \alpha', \lambda')$ be sampled from the jump chain $(Y'_t)_{t\in\mathbb{N}}$ with parameters λ' and α'. Define N'_t, M'_t, and U' analogously for the (λ', α')-chase-escape with

conversion process. We will prove the following characterization of X' that, in light of Lemma 6, implies that $X' \preceq X$.

Lemma 7. *There exists γ' such that $X'(\mathbb{N}, x_0, \alpha', \lambda') \stackrel{d}{=} N'_{\gamma'} + U'(N'_{\gamma'} - M'_{\gamma'})$ with the relations:*

(i) $N'_{\gamma'} \preceq N$
(ii) $N'_{\gamma'} - M'_{\gamma'} \preceq N - M$
(iii) $U'(n') \preceq U(n)$ *for all* $n' \leq n$.

Proof. We will proceed in two steps. First, we will produce a coupling that uses the passage time construction for trees from the previous section to prove claims (i) and (ii). The basic idea is that we take γ' to be the time the site M becomes blue in the (λ', α')-process.

In Step 2, we will proceed inductively to prove that, conditional on $Y'_t \leq Y_t$, the next step of the chain results in $Y'_{t+1} \leq Y_{t+1}$. This implies that $U'(n') \preceq U(n)$. The second step requires a minor time distortion where sometimes only one of the jump chains takes an up- or down-step while the other takes a *flat-step*. However, this does not alter the total number of up-steps taken.

Step 1: (i) and (ii). First we will formally sample M and N used to determine X in Lemma 6. As $\mathbb{N}$ is a tree graph, the passage time construction from Section 2 applies. In particular, for $y \geq 1$ we sample times $\vec{R}_{y,y+1}, \vec{B}_{y,y+1}, \hat{B}_{y+1,y}$, and C_y. Let $\mathbf{R}_1 = 0$ and, for $x \geq 2$, define $\mathbf{R}_x = \mathbf{R}_{x-1} + \vec{R}_{x-1,x}$ to be the time it takes for red to reach site x in the absence of chase and conversion. Note that $\mathbf{R}_x + C_x$ is the time it takes for site x to become red, and then convert. Define $\gamma = \min\{\mathbf{R}_x + C_x \colon x \in \mathbb{N}\}$ as the first conversion time. This minimum is realized at some almost surely unique site M. We set $N = \max\{x \colon T_x \leq \gamma\}$ to be the location of the rightmost red at time γ with the convention that $N = M$ if M is the rightmost non-white site.

For $\alpha' \geq \alpha$ and $\lambda' \leq \lambda$, sample the edges $\vec{R}'_{y,y+1}, \vec{B}'_{y,y+1}, B'_{y+1,y}$, and C'_y so that the blue spreading times are the same and $\vec{R}'_{y,y+1} \geq \vec{R}_{y,y+1}$ and $C'_y \leq C_y$. Define $\mathbf{R}'_x$ analogously using these passage times. Taking M exactly as in the previous paragraph (using the λ and α passage times), let $\gamma' = \mathbf{R}'_M + C'_M$ be the time at which site M would convert to blue using the λ' and α' passage times. We let $M'_{\gamma'}$ be the site with the rightmost blue at time γ' in the (λ', α')-process. Note that $M'_{\gamma'}$ need not equal M nor the first site to turn blue in the (λ', α')-process; it is possible that other sites were converted earlier, and even that some sites became blue from predation. We let $N'_{\gamma'}$ be the location of the rightmost red at time γ' in the (λ', α')-process with the convention that $N'_{\gamma'} = M'_{\gamma'}$ if $M'_{\gamma'}$ is the rightmost non-white site. See Figure 6 for a visual representation of these quantities.

To derive the relationship between these variables, we will first deal with the case where site M is white at time γ' in the (λ', α')-process, followed by the case when M is blue at time γ' in the (λ', α')-process. The two cases are represented in the right and left panels, respectively, of Figure 6. These are the only cases, since M cannot be red at time γ', given that γ' is the time that site M would convert from red to blue.

If M is white at time γ', then site M remains white for all time in the process with the (λ', α') passage times, and a blue site strictly to the left of M is the rightmost non-white site. Therefore, $M'_{\gamma'} = N'_{\gamma'} < M \leq N$. Therefore, $N'_{\gamma'} \leq N$ and $0 = N'_{\gamma'} - M'_{\gamma'} \leq N - M$ in this case.

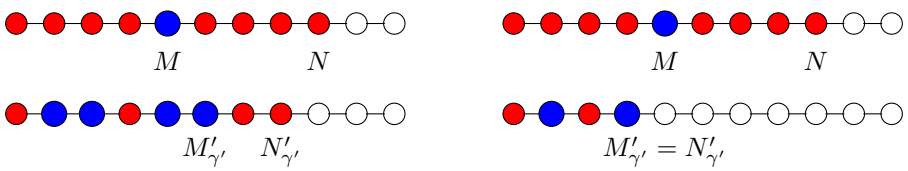

FIGURE 6. Two example realizations of chase-escape with conversion in the coupling to prove (i) and (ii) in Lemma 7. In each subfigure (left and right), the top image is the process with λ and α at time γ, and the bottom image is the process with λ' and α' at time γ'. On the left, we have $M'_{\gamma'} > M$ and $N'_{\gamma'} < N$. On the right, we have $M'_{\gamma'} = N'_{\gamma'} < N$. In both subfigures, the claimed relations $N'_{\gamma'} \leq N$ and $N'_{\gamma'} - M'_{\gamma'} \leq N - M$ hold.

Assume now that site M is blue at time γ'. In this case, $M'_{\gamma'} \geq M$, because $M'_{\gamma'}$ is the rightmost blue site and site M is blue. Since N is the location of the rightmost red site in the (λ, α)-process, it follows that

$$C_M < \sum_{i=0}^{N-M} \vec{R}_{M+i,M+i+1},$$

that is, the time that it takes red to spread from site M to site $N+1$ (at rate λ) is greater than the time it takes site M to convert to blue, at rate α. This, combined with the passage time relations $\vec{R}'_{y,y+1} \geq \vec{R}_{y,y+1}$ and $C'_y \leq C_y$, implies

$$\begin{aligned}
\gamma' &= \boldsymbol{R}'_M + C'_M \\
&\leq \boldsymbol{R}'_M + C_M \\
&< \boldsymbol{R}'_M + \sum_{i=0}^{N-M} \vec{R}_{M+i,M+i+1} \\
&\leq \boldsymbol{R}'_M + \sum_{i=0}^{N-M} \vec{R}'_{M+i,M+i+1} \\
&= \boldsymbol{R}'_{N+1}.
\end{aligned}$$

Therefore, $\gamma' < \boldsymbol{R}'_{N+1}$ and so site $N+1$ is white in the (λ', α')-process at time γ'. This implies that $N'_{\gamma'} \leq N$. Since $M'_{\gamma'} \geq M$, we have moreover $N'_{\gamma'} - M'_{\gamma'} \leq N - M$. This gives (i) and (ii).

Step 2: (iii). Let $t \geq 0$ and suppose that $Y_t = y \geq y' = Y'_t$ with $\lambda \geq \lambda'$ and $\alpha \leq \alpha'$. We will sample the next step of these chains using the Poisson edge clocks associated to the current chase-escape with conversion configuration on $\mathbb{N}$.

Adopting the convention that an Exp(0)-distributed random variable is infinite with probability one, sample the following random variables independently:

- $\tau_B \sim \text{Exp}(1)$.
- $\tau_R \sim \text{Exp}(\lambda')$ and $\sigma_R \sim \text{Exp}(\lambda - \lambda')$.
- $\tau_i \sim \text{Exp}(\alpha)$ for $i = 1, \ldots, y$, and $\sigma_i \sim \text{Exp}(\alpha' - \alpha)$ for $i = 1, \ldots, y'$.

We then set the edge transition times:

- $T_B = \tau_B = T'_B$.

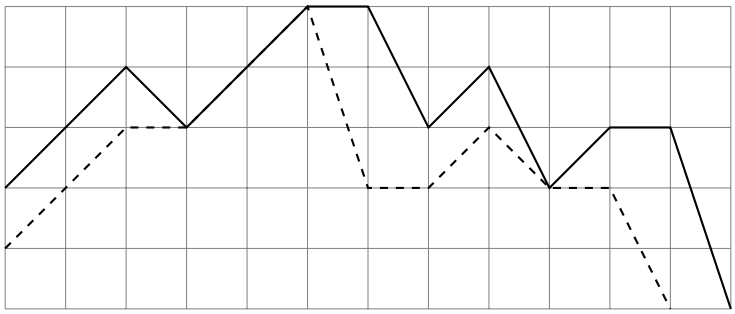

FIGURE 7. An example of the coupling in Step 2. The solid black path corresponds to Y_t with $Y_0 = 2$ and the dashed path to Y'_t with $Y'_0 = 1$. Our construction ensures $Y'_t \leq Y_t$ at all steps so long as $Y'_0 \leq Y_0$.

- $T_R = \min(\tau_R, \sigma_R)$ and $T'_R = \tau_R$.
- $T_{R,i} = \tau_i$ for $i = 1, \dots, y$ and $T'_{R,i} = \min(\tau_i, \sigma_i)$ for $i = 1, \dots, y'$.

Let

$$\tau = \min\{\tau_B, \tau_R, \sigma_R, \tau_1, \dots, \tau_y, \sigma_1, \dots, \sigma_{y'}\}.$$

Call the times $T_B, \dots, T_{R,y}$ the Y_t *edge clocks*. Similarly, the times $T'_B, \dots, T'_{R,y'}$ are the Y'_t *edge clocks*.

To obtain Y_{t+1} and Y'_{t+1}, we update the edge(s) corresponding to the edge clock(s) equal to τ. If only one edge clock updates, then the other process takes a flat step. We give the details of each situation:

- If $\tau = \tau_B$ (hence $\tau = T_B = T'_B$), then for both Y_t and Y'_t, we set the blue vertex of their respective critical regions to predate the adjacent red and so $Y_{t+1} = y - 1 \geq y' - 1 = Y'_{t+1}$.
- If $\tau = \tau_R$ (hence $\tau = T_R = T'_R$), then both Y_t and Y'_t take a *forward step* and infect their adjacent white vertices. Thus, $Y_{t+1} = y_t + 1 \geq y'_t + 1 = Y'_{t+1}$.
- If $\tau = \sigma_R$, (hence $\tau = T_R$) then we set Y_t to take a *forward step* and Y'_t to take a *flat step*. We have that $Y_{t+1} = y + 1 > y' = Y'_{t+1}$.
- If $\tau = \tau_i$ for $1 \leq i \leq y'$ (hence $\tau = T_{R,i} = T'_{R,i}$), then for both jump chains the i^{th}-red vertex (counting from the rightmost red vertex in each chain as vertex 1) converts to blue. This means that $Y_{t+1} = i - 1 = Y'_{t+1}$.
- If $\tau = \tau_i$ for $y' < i \leq y$ (hence $\tau = T_{R,i}$) we set that the i^{th}-red vertex of Y_t converts to blue (again counting from the right) and Y'_t takes a *flat step* (notice that we only defined $T'_{R,i}$ for $i = 1, \dots, y'$, so in this case, no conversion happens in the Y'_t chain). Hence, $Y_{t+1} = i - 1 \geq y' = Y'_{t+1}$.
- If $\tau = \sigma_i$ for $1 \leq i \leq y'$ (hence, $\tau = T'_{R,i}$), then we set the i^{th}-red vertex of Y'_t to convert while Y_t takes a *flat step*. Hence $Y_{t+1} = y > i - 1 = Y'_{t+1}$.

See Figure 7 for an example.

Claim 8. *Let Y be the total number of upward steps taken by $(Y_t)_{t \in \mathbb{N}}$ until reaching 0, and similarly for Y'. It holds that $Y \succeq Y'$.*

Proof. Once the flat steps are removed, this coupling gives the correct marginals for Y_t and Y'_t conditional on the values of Y_0 and Y'_0. Moreover, whenever Y'_t increases (when $\tau = \tau_R$), Y_t is coupled to increase by the same amount. Whenever

Y_t decreases, the coupling above guarantees that the Y_t chain does not fall below Y'_t. We also have cases when Y'_t moves downwards and Y_t stays fixed, and Y_t moves upwards with Y'_t fixed. Because the coupling ensures that the chains remain ordered and couples the forward steps, it is immediate that $U'_\kappa(n') \preceq U_\kappa(n)$ whenever $n' \leq n$. □

Recall that Lemma 6 states that $X(\mathbb{N}, x_0, \alpha, \lambda) = N + U_\kappa(N - M)$ and Lemma 7 that $X' = N'_{\gamma'} + U'_{\kappa'}(N'_{\gamma'} - M'_{\gamma'})$ with stochastic relations: $N'_{\gamma'} \preceq N$, $N'_{\gamma'} - M'_{\gamma'} \preceq N - M$, and $U'_{\kappa'} \preceq U_\kappa(n)$ for all $n' \leq n$. It follows that

$$X'(\mathbb{N}, x_0, \alpha', \lambda') = N'_{\gamma'} + U'_{\kappa'}(M'_{\gamma'} - N'_{\gamma'}) \preceq N + U_\kappa(N - M) = X(\mathbb{N}, x_0, \alpha, \lambda),$$

as desired. □

4. Proof of Theorem 1: Stars

For the star graph, we will return to thinking about the process in continuous time, $t \in [0, \infty)$, with the exponential clocks framework. For the star graph, the root is initially red, and red can only spread from the root. Accordingly, the number of leaves that are ever red is equal to the number of leaves in state red or blue at the time the root becomes blue.

In the following, we think of the spread of red from the root like a pure death process that starts with n individuals (representing the n white nodes), and where each one dies (here, this corresponds to becoming red) independently at rate λ. Let $\sigma(i) \in [0, \infty)$ denote the time of the i-th death with the convention that $\sigma(0) = 0$ and $\sigma(n+1) = \infty$. Note that $\sigma(i) - \sigma(i-1) \sim \text{Exp}((n-i+1)\lambda)$ for $1 \leq i \leq n$.

Similarly, let $\sigma'(i)$ denote the time of the i-th death in a coupled pure death process that starts with $n' \leq n$ individuals that each die at rate $\lambda' \leq \lambda$. Therefore, $\sigma'(i) - \sigma'(i-1) \sim \text{Exp}((n'-i)\lambda')$. Because $n' \leq n$ and $\lambda' \leq \lambda$, for each $0 \leq i \leq n'$, it is clear that $(n'-i)\lambda' \leq (n-i)\lambda$. Therefore, we couple these two processes such that

$$\sigma'(i) - \sigma'(i-1) \geq \sigma(i) - \sigma(i-1)$$

for each $0 \leq i \leq n'$. Notice that this also implies that $\sigma'(i+1) - \sigma'(k) \geq \sigma(i+1) - \sigma(k)$ for any $k \leq i \leq n'$. For $\alpha' \geq \alpha$, let $T_i \sim \text{Exp}(\alpha) + \text{Exp}(1)$ be independent and coupled with $T'_i \sim \text{Exp}(\alpha') + \text{Exp}(1)$ so that $T'_i \leq T_i$. T_i is the time it takes for the ith red leaf to convert to blue and then spread blue to the root (similarly for T'_i). Additionally, let $T_0 \sim \text{Exp}(\alpha)$ and $T'_0 \sim \text{Exp}(\alpha')$ be coupled so that $T'_0 \leq T_0$. T_0 and T'_0 represent the time it takes the root to convert to blue.

For $0 \leq i \leq n$, let

$$M_i = \min_{0 \leq k \leq i} \sigma(k) + T_k$$

and analogously for M'_i. Define

$$I = \min\{0 \leq i \leq n \colon \sigma(i+1) - M_i > 0\},$$
$$I' = \min\{0 \leq i \leq n' \colon \sigma'(i+1) - M'_i > 0\}.$$

We claim that $X = I + 1$ and $X' = I' + 1$. To see this, note that the times $\sigma(i)$ and T_i can be coupled to reflect the time red spreads to the ith leaf and the time the ith red leaf would convert the root to blue, as described above. The smallest index I such that that $\sigma(I+1) > M_I$, equivalently $\sigma(I+1) - M_I > 0$, indicates that the root has been colored blue (by one of the first I red leaves or by conversion) before the $(I+1)$th leaf turns red. So I gives how many leaves are at some point

colored red and $X = I + 1$ to account for the root. Similar reasoning gives the characterization of $X' = I' + 1$.

We may rewrite $\sigma(i+1) - M_i$ as follows

$$\begin{aligned} \sigma(i+1) - M_i &= \sigma(i+1) - \min_{0 \le k \le i} (\sigma(k) - T_k) \\ &= \max_{0 \le k \le i} (\sigma(i+1) - \sigma(k) - T_k) \end{aligned} \tag{5}$$

Recall that from our coupling, we have that for all $0 \le k \le i$

$$\sigma(i+1) - \sigma(k) \le \sigma'(i+1) - \sigma'(k),$$

so

$$\sigma(i+1) - \sigma(k) - T_k \le \sigma'(i+1) - \sigma'(k) - T_k.$$

Similarly by the coupling, because $T_k \ge T'_k$, we also have that

$$\sigma(i+1) - \sigma(k) - T_k \le \sigma'(i+1) - \sigma'(k) - T'_k.$$

Therefore, for $0 \le i \le n'$,

$$\max_{0 \le k \le i} (\sigma(i+1) - \sigma(k) - T_k) \le \max_{0 \le k \le i} (\sigma'(i+1) - \sigma'(k) - T'_k),$$

which by (5) implies that

$$\sigma(i+1) - M_i \le \sigma'(i+1) - M'_i. \tag{6}$$

Suppose now that $I = i$ with $0 \le i \le n'$. Then $0 < \sigma(i+1) - M_i$, and by (6)

$$0 < \sigma(i+1) - M_i \le \sigma'(i+1) - M'_i.$$

which yields $I' \le i = I$. On the other hand, if $I = i$ with $i > n'$, then $I' \le n' < i = I$. Since $X = I + 1$ and $X' = I' + 1$, this proves that $X' \preceq X$.

Remark 9. *We point out that the passage time for construction of X on trees in Section 2 does not appear to easily give monotonicity of X in λ and n if one simply couples the passage times for the (λ, α, n) and (λ', α', n') processes in the canonical way. Without the further coupling we give here, of assigning the conversion time and then predation of the root dynamically, it is possible that speeding up an edge passage time or adding a new edge could dramatically reduce X compared to X'.*

5. Proof of Theorem 1: The complete graph

As with S_n, it is more convenient to work in continuous time $t \in [0, \infty)$ using the exponential clocks in the definition of chase-escape with conversion. Let $(R_t)_{t \in \mathbb{N}}$ be the number of vertices in state r at time t. Similarly, let $(B_t)_{t \in \mathbb{N}}$ be the number of blue vertices. Let $W_t = n - R_t - B_t$ be the number of vertices in state w. Conditional on $R_t = r, B_t = b$, and $W_t = w = n - (r + b)$, we have the following transition probabilities at the next jump time:

$$p^+_{r,b} = \frac{\lambda w r}{\lambda r w + b r + \alpha r}; \quad p^-_{r,b} = \frac{b r + \alpha r}{\lambda r w + b r + \alpha r},$$

where $p^+_{r,b}$ is the probability R_t increases by 1 and $p^-_{r,b}$ is the probability R_t decreases by one while B_t increases by 1. As observed for chase-escape on the complete graph in [15], r is common to all summands and can thus be factored and canceled. The common r term persists with conversion. Hence, for all $1 \le r \le n$ we have

$$p^+_{r,b} := \frac{\lambda w}{\lambda w + b + \alpha}; \quad p^-_{r,b} := \frac{b+\alpha}{\lambda w + b + \alpha}. \tag{7}$$

[15, Theorem 1.1] uses this observation to deduce that the number of sites ever infected by red can be characterized by a simple process involving independent pure birth and pure death processes. This is still true in chase-escape with conversion, but with the addition of constant immigration to the birth process. We describe these processes below.

The death process starts with $n-1$ individuals, each of which die at exponential rate λ. Let $\mathcal{W}_t$ denote the number of individuals remaining at time t. The birth process starts with 0 individuals who generate an additional individual at exponential rate 1. Additionally, there is a constant immigration process where a new individual is added at exponential rate α (that does not depend on the population size). Let $\mathcal{B}_t$ denote the number of individuals at time t. Additionally, let $\sigma(i)$ denote the time (in continuous units) of the ith jump in the death process and $\rho(i)$ denote the time of the ith jump in the birth process. By construction, $\sigma(i+1)-\sigma(i) \sim \mathrm{Exp}(\lambda(n-1-i))$ for $0 \le i \le n-2$ and $\rho(i+1)-\rho(i) \sim \mathrm{Exp}(i+\alpha)$ for $i \ge 0$.

One can check that $\mathcal{W}_t$ at its jumps corresponds to W_t and $\mathcal{B}_t$ tracks B_t (with a time change, since we have removed the scaling corresponding to R_t). This is true because the transition probabilities for either chain are given by (7). Letting

$$\rho_* := \rho(\min\{i \ge 1 \colon \rho(i) < \sigma(i)\}),$$

this correspondence holds up to the stopping time

$$\tau = \sigma(n-1) \wedge \rho_*$$

at which point either no white or no red vertices remain. We can use this coupling to characterize X as:

$$X(K_n, x_0, \alpha, \lambda) = n - \mathcal{W}_\tau.$$

We obtain monotonicity of X in λ, α, and n by virtue of this coupling. To go into more detail, increasing λ speeds up the jump times $\sigma(i)$, this stochastically increases ρ_*, thus decreasing $\mathcal{W}_\tau$ and increasing X. On the other hand, increasing α speeds up the jump times $\rho(i)$, which stochastically decreases ρ_*, thus increasing $\mathcal{W}_\tau$ and decreasing X. Lastly, increasing n speeds up the jump times $\sigma(i)$, thus this increases ρ_*, which results in a stochastic increase to X.

Remark 10. *An interesting future inquiry is generalizing the results from* [15] *to chase-escape with conversion. The main difference is the constant immigration at rate α, which appears to have a non-trivial impact on the key tool that pure birth and death processes are representable as time changes of unit Poisson processes.*

6. Proof of Theorem 2

In this section, we will take $\alpha > 0$ to be fixed and indicate the dependence of the measure $\mathbf{P}$ on λ with a subscript $\mathbf{P}_\lambda$. First we prove the lower bound. We proceed by showing the stronger statement that $\mathbf{E}_\lambda[X] < \infty$ for sufficiently small λ. Let Γ_k be the set of all vertex self-avoiding paths of length k starting at x_0 that are present in G. Interpret $\Gamma_0 = (x_0)$ as the path of length 0 starting at x_0. We say that red *survives* on a path $\gamma \in \Gamma_k$ if, for chase-escape with conversion restricted only to the passage times along γ, the terminal vertex of γ is at some point colored

red. We emphasize that survival along γ ignores the influence of red and blue from all edges not belonging to γ.

Let $A_k = A_k(\lambda)$ be the event that k is ever colored red in chase-escape with conversion on the infinite path $0, 1, 2, \dots$ with 0 initially red. Observe that

$$\mathbf{P}_\lambda(\text{red survives on a path } \gamma \text{ of length } k) = \mathbf{P}_\lambda(A_k).$$

A necessary condition for A_k is that at each site $i = 0, 1, \dots, k-1$, red spreads from i to $i+1$ before i converts to blue. This happens with probability $\lambda/(\lambda+\alpha)$ independently at each site. Thus,

$$\mathbf{P}_\lambda(A_k) \leq \left(\frac{\lambda}{\lambda+\alpha}\right)^k.$$

Let $H \subseteq G$ denote the set of sites that are ever colored red, so that $X = |H|$. For any vertex $v \in H$ there must be a path along which red survives with v the terminal point. Hence,

$$X \preceq \sum_{k=0}^{\infty} \sum_{\gamma \in \Gamma_k} \mathbf{1}\{\text{red survives on } \gamma\}.$$

Taking expectation and using the bound on $\mathbf{P}_\lambda(A_k)$ plus the fact that $|\Gamma_0| = 1$ and $|\Gamma_k| \leq d(d-1)^{k-1}$ for $k \geq 1$ gives

$$\mathbf{E}_\lambda[X] \leq \sum_{k=0}^{\infty} |\Gamma_k| \mathbf{P}_\lambda(A_k) \leq 1 + \frac{d\lambda}{\lambda+\alpha} \sum_{k=0}^{\infty} \left(\frac{(d-1)\lambda}{\lambda+\alpha}\right)^k.$$

This quantity is finite so long as $(d-1)\lambda/(\lambda+\alpha) < 1$, which holds for $\lambda < \alpha/(d-2)$.

Now we prove the upper bound on $\lambda_c(\alpha)$. We will use here the notation of defining the process through random variables associated to directed edges which was introduced in Section 2. For each vertex $x \in G$, let $\mathcal{N}(x)$ be the collection of vertices connected to x. As a reminder of the necessary notation, recall that for any vertex $x \in G$ and y a neighbor of x, $y \in \mathcal{N}(x)$, we define $\mathcal{E}_{x,y}$ to be the directed edge connecting x to y and $\mathcal{E}_{y,x}$ as the directed edge connecting y to x. As before, we assign the random variable $\vec{R}_{x,y}$ to the edge $\mathcal{E}_{x,y}$, which defines the time until red spreads from x to y and the random variable $\vec{B}_{y,x}$ to the edge $\mathcal{E}_{y,x}$ to be the time until blue spreads from y to x. Let C_x be the time until vertex x converts from red to blue. With this notation in place, we call a vertex $x \in G$ *good* if

$$\max_{y \in \mathcal{N}(x)} \vec{R}_{x,y} < \min_{y \in \mathcal{N}(x)} \vec{B}_{y,x} \wedge C_x.$$

In words, this means that a vertex x is good if the time it would take to spread red to all its neighboring sites is less than the shortest possible length of time after x becomes red before blue can affect the site, either through conversion or spreading.

If $\mathcal{C}$ is the connected component of good sites containing x_0, it is easy to deduce that all sites of $\mathcal{C}$ will at some point be colored red. This is because red spreads to all of its neighbors from each site in $\mathcal{C}$ before being affected by blue. Thus, $X \succeq |\mathcal{C}|$. We then have $\mathbf{P}_\lambda(X = \infty) \geq \mathbf{P}_\lambda(|\mathcal{C}| = \infty)$. Recall that $p_c = p_c(G)$ is the critical threshold for Bernoulli site percolation on G. It suffices to show that for each $x \in G$, $\mathbf{P}_\lambda(x \text{ is good}) > p_c$ for λ sufficiently large as this implies that $\mathbf{P}_\lambda(X = \infty) > 0$.

The probability a given site x is good is the probability the maximum of $|\mathcal{N}(x)|$ independent $\text{Exp}(\lambda)$ random variables is smaller than the minimum of $|\mathcal{N}(x)|$ independent $\text{Exp}(1)$ random variables and one independent $\text{Exp}(\alpha)$ random variables.

Because $|\mathcal{N}(x)| \leq d$, the probability x is good is bounded below by the probability that R_d, the maximum of d independent $\text{Exp}(\lambda)$ random variables, is smaller than B_d, the minimum of d independent $\text{Exp}(1)$ random variables and one independent $\text{Exp}(\alpha)$ random variable. Thus,

$$\mathbf{P}_\lambda(x \text{ is good}) \geq \mathbf{P}_\lambda(R_d < B_d) = \int_0^\infty \mathbf{P}_\lambda(R_d < z) f_{B_d}(z) dz,$$

where $f_{B_d}(z)$ is the density of B_d.

We would like to find a condition on λ that ensures this integral is strictly larger than p_c. One way to do this is to note that $R_d \preceq R'_d \sim \text{Gamma}(d, \lambda)$ i.e. the sum of d independent $\text{Exp}(\lambda)$ random variables, since the maximum of d independent $\text{Exp}(\lambda)$ random variables is bounded by the sum. This has a simpler formulation

$$\mathbf{P}_\lambda(x \text{ is good}) \geq \mathbf{P}_\lambda(R'_d < B_d) = \left(\frac{\lambda}{\lambda + d + \alpha}\right)^d.$$

The formula is easily derived from iteratively applying the memoryless property of the exponential distribution since each of the d independent $\text{Exp}(\lambda)$ random variables in the sum comprising R'_d must occur before the $\text{Exp}(d + \alpha)$-distributed random variable B_d.

Letting $p = p_c$, some algebra then gives that

$$\lambda > \frac{p^{\frac{1}{d}}(d + \alpha)}{1 - p^{\frac{1}{d}}} \implies \left(\frac{\lambda}{\lambda + d + \alpha}\right)^d > p.$$

Replacing $p^{1/d}$ with 1 in the numerator on the left yields that whenever $\lambda \geq (d + \alpha)/(1 - p^{1/d})$ we have $\mathbf{P}_\lambda(X = \infty) > 0$. Thus, $\lambda_c(\alpha)$ is no larger than $(d+\alpha)/(1 - p^{1/d})$.

References

[1] Erin Beckman, Keisha Cook, Nicole Eikmeier, Saraí Hernández-Torres, and Matthew Junge. Chase-escape with death on trees. *The Annals of Probability*, 49(5):2530–2547, 2021.

[2] Emma Bernstein, Clare Hamblen, Matthew Junge, and Lily Reeves. Chase-escape on the configuration model. *Electronic Communications in Probability*, 27:1–14, 2022.

[3] Charles Bordenave. On the birth-and-assassination process, with an application to scotching a rumor in a network. *Electronic Journal of Probability*, 13:2014–2030, 2008.

[4] Charles Bordenave. Extinction probability and total progeny of predator-prey dynamics on infinite trees. *Electronic Journal of Probability*, 19(20):1–33, 2014.

[5] Giancarlo Comi, Massimo Filippi, Jerry S Wolinsky, and European/Canadian Glatiramer Acetate Study Group. European/canadian multicenter, double-blind, randomized, placebo-controlled study of the effects of glatiramer acetate on magnetic resonance imaging–measured disease activity and burden in patients with relapsing multiple sclerosis. *Annals of neurology*, 49(3):290–297, 2001.

[6] Guilherme Ferraz de Arruda, Elcio Lebensztayn, Francisco A Rodrigues, and Pablo Martín Rodríguez. A process of rumour scotching on finite populations. *Royal Society Open Science*, 2(9):150240, 2015.

[7] Ruth Dobson and Gavin Giovannoni. Multiple sclerosis–a review. *European Journal of Neurology*, 26(1):27–40, 2019.

[8] Rick Durrett. *Random graph dynamics*, volume 20. Cambridge university press, 2010.

[9] Rick Durrett, Matthew Junge, and Si Tang. Coexistence in chase-escape. *Electronic Communications in Probability*, 25:1–14, 2020.

[10] Alexander Hinsen, Benedikt Jahnel, Elie Cali, and Jean-Philippe Wary. Phase transitions for chase-escape models on Poisson–Gilbert graphs. *Electronic Communications in Probability*, 25(none):1 – 14, 2020.

[11] William R Holmes and Qing Nie. Interactions and tradeoffs between cell recruitment, proliferation, and differentiation affect cns regeneration. *Biophysical journal*, 106(7):1528–1536, 2014.

[12] Geoffrey D. Keeler, Sandeep Kumar, Brett Palaschak, Emily L. Silverberg, David M. Markusic, Noah T. Jones, and Brad E. Hoffman. Gene therapy-induced antigen-specific tregs inhibit neuro-inflammation and reverse disease in a mouse model of multiple sclerosis. *Molecular Therapy*, 26(1):173–183, 2018.

[13] Matthew James Keeling. *The ecology and evolution of spatial host-parasite systems*. PhD thesis, University of Warwick, 1995.

[14] Taehyong Kim, Woo-Chang Hwang, Aidong Zhang, Murali Ramanathan, and Surajit Sen. Damage isolation via strategic self-destruction: A case study in 2d random networks. *Europhysics Letters*, 86(2):24002, 2009.

[15] Igor Kortchemski. A predator-prey SIR type dynamics on large complete graphs with three phase transitions. *Stochastic Processes and their Applications*, 125(3):886 – 917, 2015.

[16] Ekaterina Kotelnikova, Marti Bernardo-Faura, Gilad Silberberg, Narsis A Kiani, Dimitris Messinis, Ioannis N Melas, Laura Artigas, Elena Schwartz, Ilya Mazo, and Mar Masso. Signaling networks in MS: a systems-based approach to developing new pharmacological therapies. *Multiple Sclerosis Journal*, 21(2):138–146, 2015.

[17] Aanjaneya Kumar, Peter Grassberger, and Deepak Dhar. Chase-escape percolation on the 2d square lattice. *Physica A: Statistical Mechanics and its Applications*, page 126072, 2021.

[18] Hans Lassmann, Jack Van Horssen, and Don Mahad. Progressive multiple sclerosis: pathology and pathogenesis. *Nature Reviews Neurology*, 8(11):647–656, 2012.

[19] MC Lombardo, R Barresi, E Bilotta, F Gargano, P Pantano, and M Sammartino. Demyelination patterns in a mathematical model of multiple sclerosis. *Journal of mathematical biology*, 75(2):373–417, 2017.

[20] Fred D Lublin, Stacey S Cofield, Gary R Cutter, Robin Conwit, Ponnada A Narayana, Flavia Nelson, Amber R Salter, Tarah Gustafson, Jerry S Wolinsky, and CombiRx Investigators. Randomized study combining interferon and glatiramer acetate in multiple sclerosis. *Annals of neurology*, 73(3):327–340, 2013.

[21] Ra Mathankumar and TR Krishna Mohan. Autoimmune control of lesion growth in cns with minimal damage. *The European Physical Journal Special Topics*, 222(3):769–776, 2013.

[22] A Reaction-Diffusion Model. for relapsing-remitting multiple. In *Numerical Mathematics and Advanced Applications ENUMATH 2023, Volume 2: European Conference, September 4-8, Lisbon, Portugal*, volume 154, page 430. Springer Nature, 2025.

[23] Nicolae Moise and Avner Friedman. A mathematical model of the multiple sclerosis plaque. *Journal of Theoretical Biology*, 512:110532, 2021.

[24] DA Rand, Matthew Keeling, and HB Wilson. Invasion, stability and evolution to criticality in spatially extended, artificial host—pathogen ecologies. *Proceedings of the Royal Society of London. Series B: Biological Sciences*, 259(1354):55–63, 1995.

[25] Menno M Schoonheim, Tommy AA Broeders, and Jeroen JG Geurts. The network collapse in multiple sclerosis: An overview of novel concepts to address disease dynamics. *NeuroImage: Clinical*, 35:103108, 2022.

[26] Si Tang, George Kordzakhia, and Steven P. Lalley. Phase Transition for the Chase-Escape Model on 2D Lattices. *arXiv:1807.08387*, July 2018.

[27] Krishna Mohan Thamattoor Raman. Simulation of spread and control of lesions in brain. *Computational and Mathematical Methods in Medicine*, 2012(1):383546, 2012.

[28] Ludovica Luisa Vissat, Jane Hillston, and Anna Williams. Modelling the remyelination process as a spatial stochastic system. Unpublished.

[29] Georgia Weatherley, Robyn P Araujo, Samantha J Dando, and Adrianne L Jenner. Could mathematics be the key to unlocking the mysteries of multiple sclerosis? *Bulletin of Mathematical Biology*, 85(8):75, 2023.

University of Bristol
Email address: e.c.bailey@bristol.ac.uk

Utah State University
Email address: erin.beckman@usu.edu

Universidad Nacional Autónoma de México
Email address: saraiht@im.unam.mx

Baruch College
Email address: Matthew.Junge@baruch.cuny.edu

Sante Fe Institute
Email address: aanjaneya@santafe.edu

Hunter College
Email address: annleeny9@gmail.com

Baruch College
Email address: danny.li2@baruchmail.cuny.edu

Hunter College and Columbia University
Email address: taqueer@proton.me

Baruch College
Email address: alisherkhon.raufov@baruchmail.cuny.edu

California Institute of Technology
Email address: lreeves@caltech.edu

Baruch College
Email address: omer.rondel@baruchmail.cuny.edu